

Supporting Information

Single-molecule analysis of interaction between p53TAD and MDM2 using aerolysin nanopores

Sohee Oh,^{ab} Mi-Kyung Lee*^{ab}, and Seung-Wook Chi*^{ab}

^a Disease Target Structure Research Center, Division of Biomedical Research, Korea Research Institute of Bioscience and Biotechnology, Daejeon 34141, Republic of Korea.

^b Department of Proteome Structural Biology, KRIBB School of Bioscience, University of Science and Technology, Daejeon 34113, Republic of Korea.

*Email: miki@kribb.re.kr; swchi@kribb.re.kr

Table of Contents

Experimental details

1. Preparation of materials
2. Preparation of aerolysin
3. Single-channel recording
4. Nanopore data analysis

Fig. S1. Comparison of the nanopore events obtained from p53_{TAD1} and E₅-p53_{TAD1}

Fig. S2. Long-lived events of the E₅-p53_{TAD1}/MDM2 complex

Fig. S3. Determination of event frequency (f) and τ_{on} values of free E₅-p53_{TAD1} and complexes.

Fig. S4. Determination of binding affinity (K_d) of the E₅-p53_{TAD1}-MDM2 interaction.

Fig. S5. Scatter plots of nanopore events from E₅-pT18-p53_{TAD1} with/without MDM2.

Fig. S6. Voltage dependency of nanopore events from E₅-pT18-p53_{TAD1}

Fig. S7. Determination of event frequency (f) and τ_{on} values of free E₅-pT18-p53_{TAD1} and complexes.

Fig. S8. Inhibitory effect of Nutlin-3 on the interaction between the E₅-p53_{TAD1} and MDM2

Fig. S9. Inhibitory effect of AMG232 on the interaction between the E₅-p53_{TAD1} and MDM2

Fig. S10. Effect of the nonbinder control, LCL161 on the interaction between E₅-p53_{TAD1} and MDM2

Fig. S11. Scatter plots of nanopore events of the E₅-p53_{TAD1}/MDM2 complex in the absence and presence of small molecule inhibitors

Fig. S12. Nanopore current traces of E₅-p53_{TAD1} and 1:1 E₅-p53_{TAD1}/MDM2 complex at the concentrations of 5 nM and 10 nM.

Experimental details

1. Preparation of materials

MDM2 (residues 3–109, PDB code: 1YCR) construct was expressed in *E. coli* BL21 (DE3) by induction with 0.4 mM isopropyl- β -D-thiogalactoside (IPTG) at an OD₆₀₀ of 0.9, and incubated overnight at 20 °C. The protein was initially purified by ammonium sulfate-induced precipitation. Further purification was carried out using HiTrap™ Q- and SP-Sepharose columns (GE Healthcare, Chicago, IL, USA) and a gel filtration column (HiLoad 16/600 Superdex 75 pg, GE healthcare, Chicago, IL, USA). p53_{TAD1} (NH₂-SQETFSDLWKLLEN-COOH) and E₅-p53_{TAD1} (NH₂-EEEEESQETFSDLWKLLEN-COOH) peptides were purchased from Peptron Inc. (Daejeon, Republic of Korea). The small-molecules Nutlin-3 (581.5 g/mol, Cayman Chemical Inc., Ann Arbor, MI, USA), AMG232 (568.55 g/mol, Cayman Chemical Inc., Ann Arbor, MI, USA), and LCL161 (500.63 g/mol, selleckchem.com, Houston, TX, USA) were commercially obtained. For E₅-p53_{TAD1}/MDM2 complex formation, the samples were incubated at 25°C for 3h in 25 mM MES (pH 6.5) buffer with 150 mM NaCl and 2 mM DTT and then added to the cis compartment at a final concentration of 1 μ M (up to 1:6 complex) for nanopore experiments. To detect PPI inhibition, we added small-molecule MDM2 inhibitors (Nutlin-3 and AMG232) and a negative control (LCL161) to 1:3 E₅-p53_{TAD1}/MDM2 complex (mixture of 1 μ M E₅-p53_{TAD1} and 3 μ M MDM2) at the molar ratios of 1:3:1, 1:3:2, and 1:3:5.

2. Preparation of aerolysin

Proaerolysin (wild-type) was expressed using pET21a vector (C-terminal 6xHis tag) in *E. coli* BL21(DE3) pLysS cell. Protein expression was induced by 0.25 mM IPTG at an OD₆₀₀ of 0.6, and grown at 16 °C for 2 h. The cells were lysed using a buffer of 0.1 M Tris-HCl pH 8.0, 18% sucrose, 5 mM EDTA, and 0.2 mg/mL lysozyme. After agitation at 4°C for 30 min using a rotator, the supernatants and pellets were separated by high-speed centrifugation at 14,000 rpm for 2 h at 4 °C. The supernatant was purified using a HisTrap™ column (GE Healthcare, Chicago, IL, USA) with elution buffer containing 20 mM sodium phosphate pH 7.4, 0.5 M NaCl, and 0.5 M imidazole. Finally, the protein was dialyzed against 10 mM Tris-HCl (pH 8.0) buffer containing 20 mM EDTA. To obtain activated aerolysin, proaerolysin was incubated with trypsin-agarose beads (1:50 v/v) (Sigma-Aldrich, St. Louis, MO, USA) for 4 h at 25°C. The trypsin-agarose beads were removed by centrifugation at 10,000 g for 15 min at 25°C. The activated aerolysin protein solution was stored at -20 °C.

3. Single-channel recording

A lipid-bilayer membrane of 3% (w/v) 1,2-Diphytanoyl-sn-glycero-3-phosphocholine (DPhPC, Avanti Polar Lipids, Inc., Alabaster, AL, USA) in decane was formed over a 50–100- μ m aperture in diameter in the center of the Teflon film that partitioned between the *cis* and *trans* compartments. The customized Teflon chambers were connected to an Ag/AgCl electrode and patch clamp amplifier system (Axopatch 200B) equipped with a Digidata 1550B A/D converter (Molecular Devices Inc., Sunnyvale, CA, USA). The *cis* compartment contained

10 mM Tris-HCl (pH 8.0), 1 mM EDTA, and 200 mM KCl. For the salt-gradient measurement, the *trans* compartment contained 10 mM Tris-HCl (pH 8.0), 1 mM EDTA, and 1 M KCl. The aerolysin was added to the *cis* compartment at an applied potential of 200 mV. Once a stable single aerolysin nanopore was formed, the free analyte and the complex solution were added to the *cis* compartment. Nanopore events were monitored at an applied potential of 80 to 160 mV using pClamp 11 software (Molecular Devices Inc., Sunnyvale, CA, USA). The current signal was filtered with a low-pass Bessel filter at 5 kHz with additional filtering at 2 kHz and acquired at a sampling rate of 250 kHz. All nanopore experiments were performed at 25 °C.

4. Nanopore data analysis

Nanopore data were analyzed using Clampfit (Molecular Devices Inc., Sunnyvale, CA, USA). The current blockade is described as I_{res}/I_0 , where I_{res} and I_0 are the residual current for the analyte and open pore current, respectively. The mean values of current blockades and dwell times were calculated from the peak values in the histograms fitted to a Gaussian function or a single exponential decay function. Standard deviation errors are based on three independent nanopore experiments (n=3). All graphs and corresponding fits were plotted using OriginPro 2020 software (OriginLab Corporation, Northampton, MA, USA). Nanopore data of the E₅-p53_{TAD1} peptide-MDM2 complex rarely showed extremely long-lived events with dwell times > 2 min, accounting for 0.2 % of total nanopore events. To clarify the statistical relevance, we analyzed nanopore events excluding extremely long-lived events with dwell times > 2 min.

To determine the binding affinity (K_d) determination of E₅-p53_{TAD1}/MDM2 interaction, we analyzed event frequencies of E₅-p53_{TAD1} (1 μM) with titration of MDM2 (up to 6 μM). The decrease in the event frequency of free E₅-p53_{TAD1} was proportional to the concentration of MDM2 (Fig. 3). The complex formation of E₅-p53_{TAD1}/MDM2 was saturated at the titration of 6 μM MDM2 ($f_{\text{min}} = \sim 0.449$). Based on the independent three nanopore measurement of each titration, we determined the normalized bound fraction (N_{fb}) of the E₅-p53_{TAD1}/MDM2 complex at each titration using the following equation:

$$N_{\text{fb}} = 1 - \frac{f - f_{\text{min}}}{f_{\text{max}} - f_{\text{min}}}$$

where f_{max} and f_{min} are event frequencies of E₅-p53_{TAD1} in the absence of MDM2 and at the saturated concentration of MDM2, respectively. The bound fraction was plotted against the concentration of MDM2 and the data were fitted to a Hill function with the Hill coefficient set to 1 (Fig. S4).

To determine the lowest concentration of protein sample for nanopore detection, we tested nanopore measurements with 5 nM and 10 nM samples of free E₅-p53_{TAD1} and 1:1 complexes (Fig. S12).

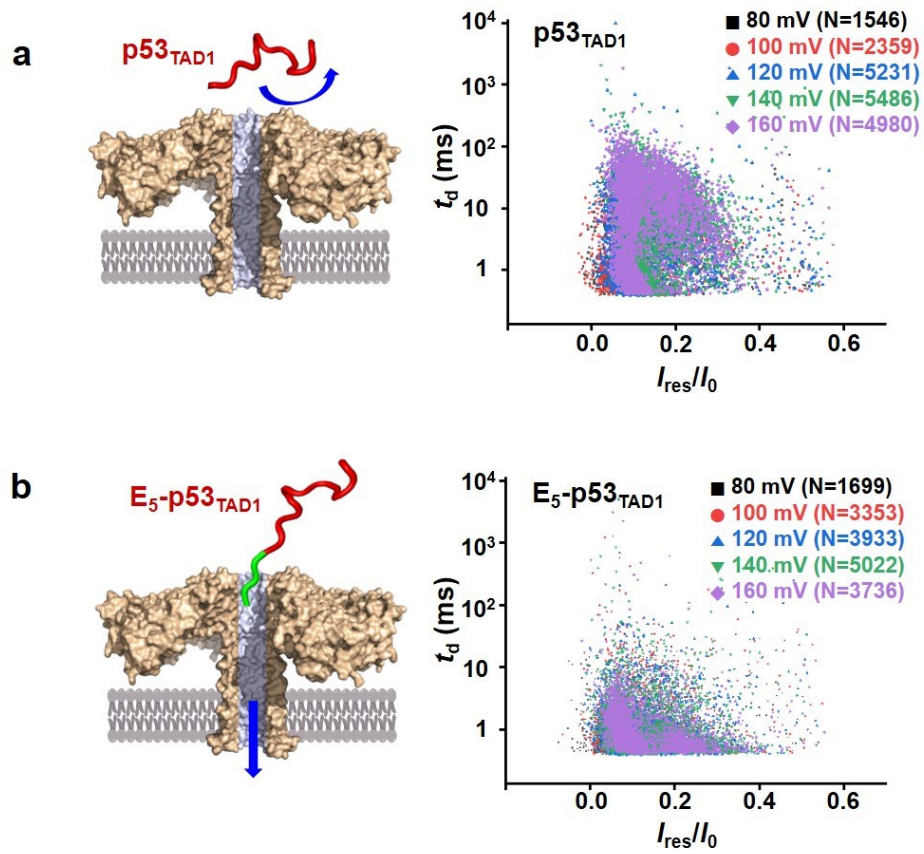


Fig. S1. Comparison of the nanopore events obtained from $p53_{TAD1}$ and E_5-p53_{TAD1} . Illustration and scatter plots of the nanopore events of $p53_{TAD1}$ (a) and E_5-p53_{TAD1} (b).

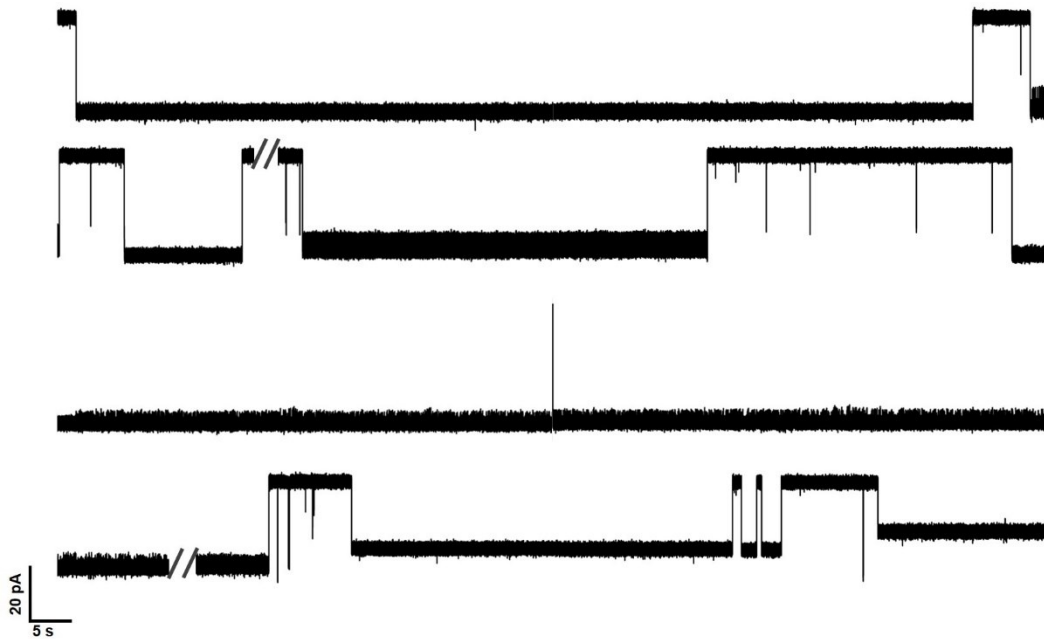


Fig. S2. Long-lived events of the E_5 -p53_{TAD1}/MDM2 complex. Selected extraordinarily long-lived events in the current traces (50 min) of the E_5 -p53_{TAD1}/MDM2 complex (at the molar ratio of 1:3) at an applied voltage of 140 mV.

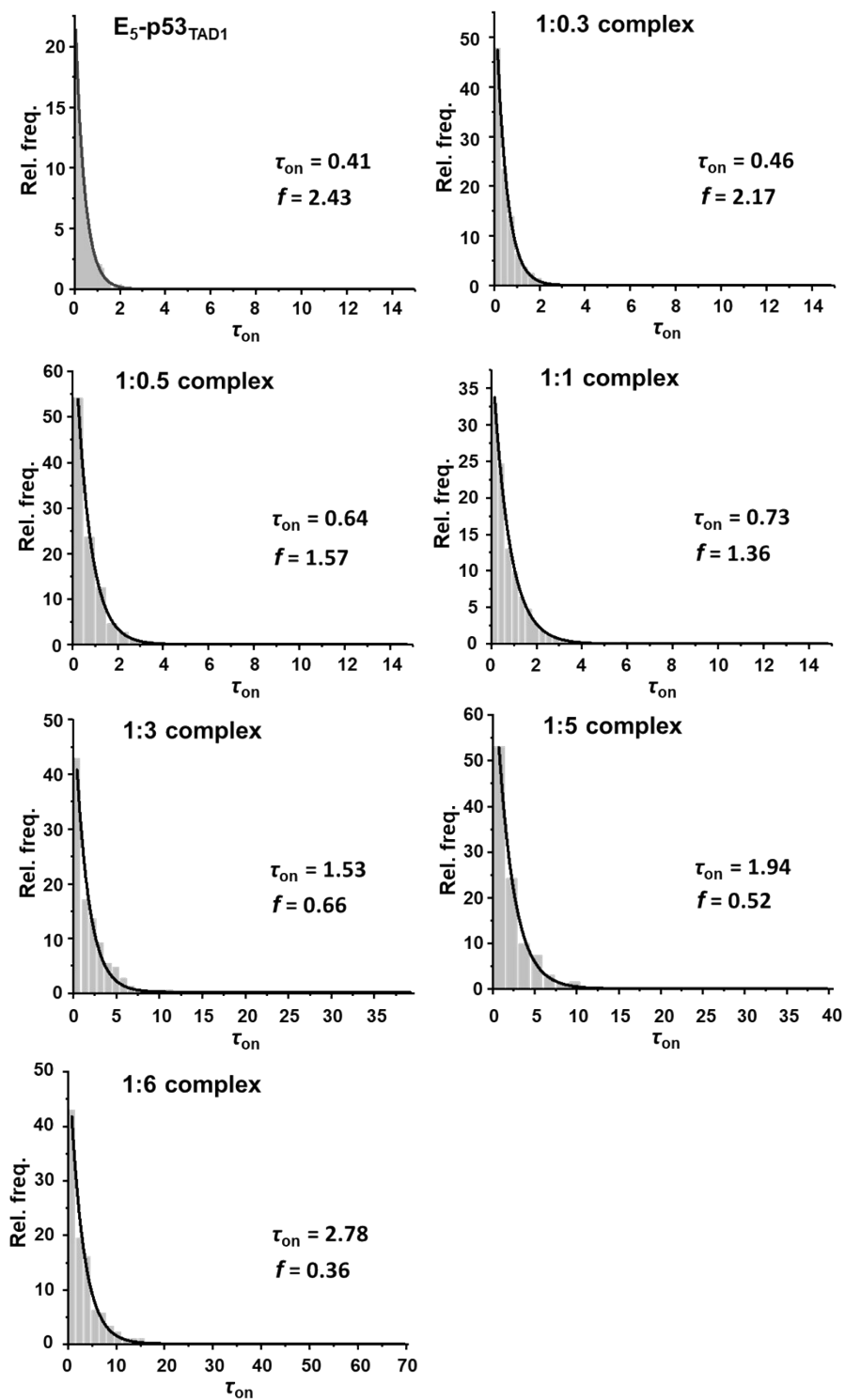


Fig. S3. Determination of event frequency (f) and τ_{on} values of free E₅-p53_{TAD1} and complexes. The τ_{on} values were determined by fitting to exponential decay. The bin values were 0.1 – 1.6. The number of bins were 27 – 150.

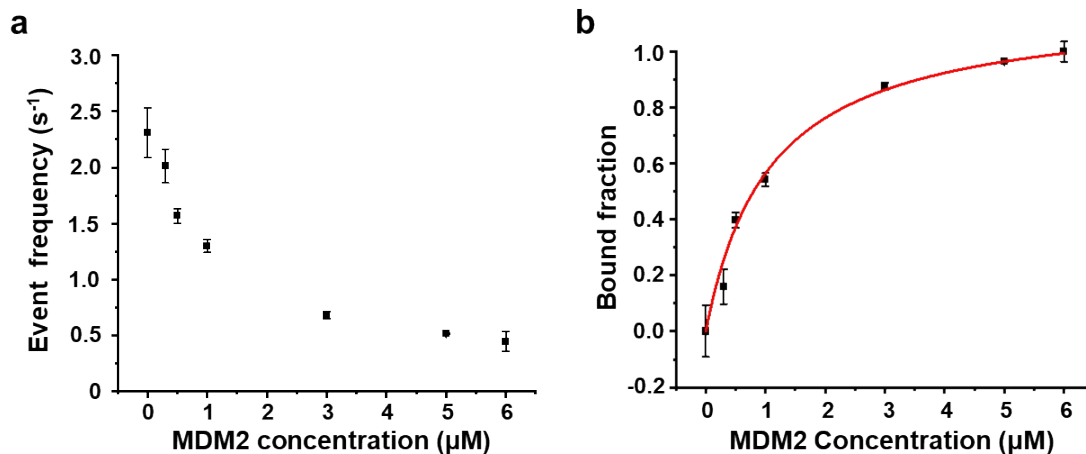


Fig. S4. Determination of binding affinity (K_d) of E_5 -p53_{TAD1}-MDM2 interaction. (a) Changes in nanopore event frequency of the free E_5 -p53_{TAD1} according to the MDM2 concentration. The error bar indicates the standard deviation based on at least three independent experiments. The event frequencies were calculated using $f=1/\tau_{on}$, where τ_{on} represents the inter-event interval. The value of τ_{on} at each MDM2 concentration was determined by fitting to a single exponential decay function (bin = 0.1 – 1.6). (b) Bound fraction was determined based on normalized fraction of event frequencies of free peptide and complexes. The determined K_d value was $1.07 \pm 0.09 \mu\text{M}$. The standard deviations of event frequencies are based on three independent nanopore measurements.

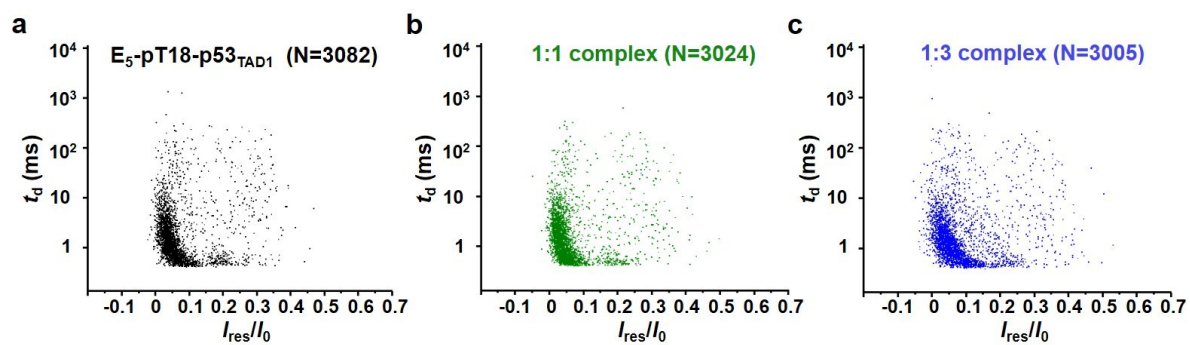


Fig. S5. Scatter plots of nanopore events from E_5 -pT18-p53_{TAD1} with or without MDM2. Scatter plots of nanopore events from free E_5 -pT18-p53_{TAD1} (a), with MDM2 protein at the 1:1 (b), and 1:3 (c) molar ratios and an applied voltage of 140 mV.

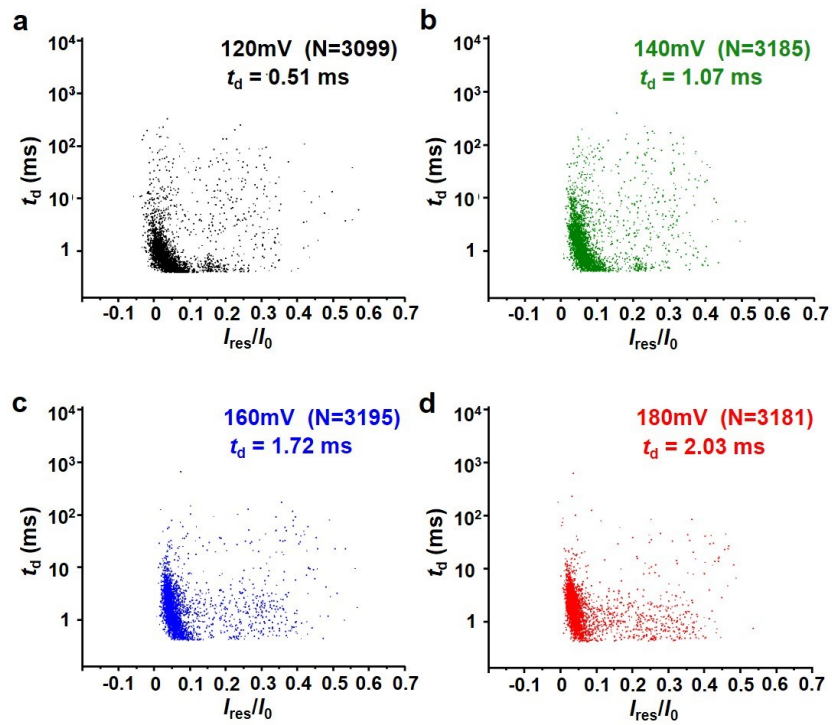


Fig. S6. Voltage dependency of nanopore events from E₅-pT18-p53_{TAD1}. Scatter plots of nanopore events obtained at 120 mV (a), 140 mV (b), 160 mV (c), and 180 mV (d). The mean value (t_d) of dwell times was determined by fitting to a single exponential decay function. The bin values are 0.5 to 1.

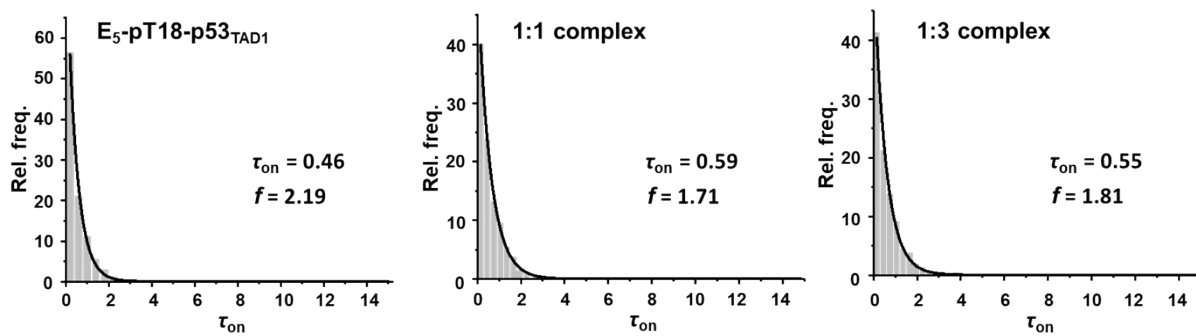


Fig. S7. Determination of event frequency (f) and τ_{on} values of free E_5 -pT18-p53_{TAD1} and complexes. The τ_{on} values were determined by fitting to exponential decay. The bin values were 0.3 – 0.4. The number of bins were 38 – 50.

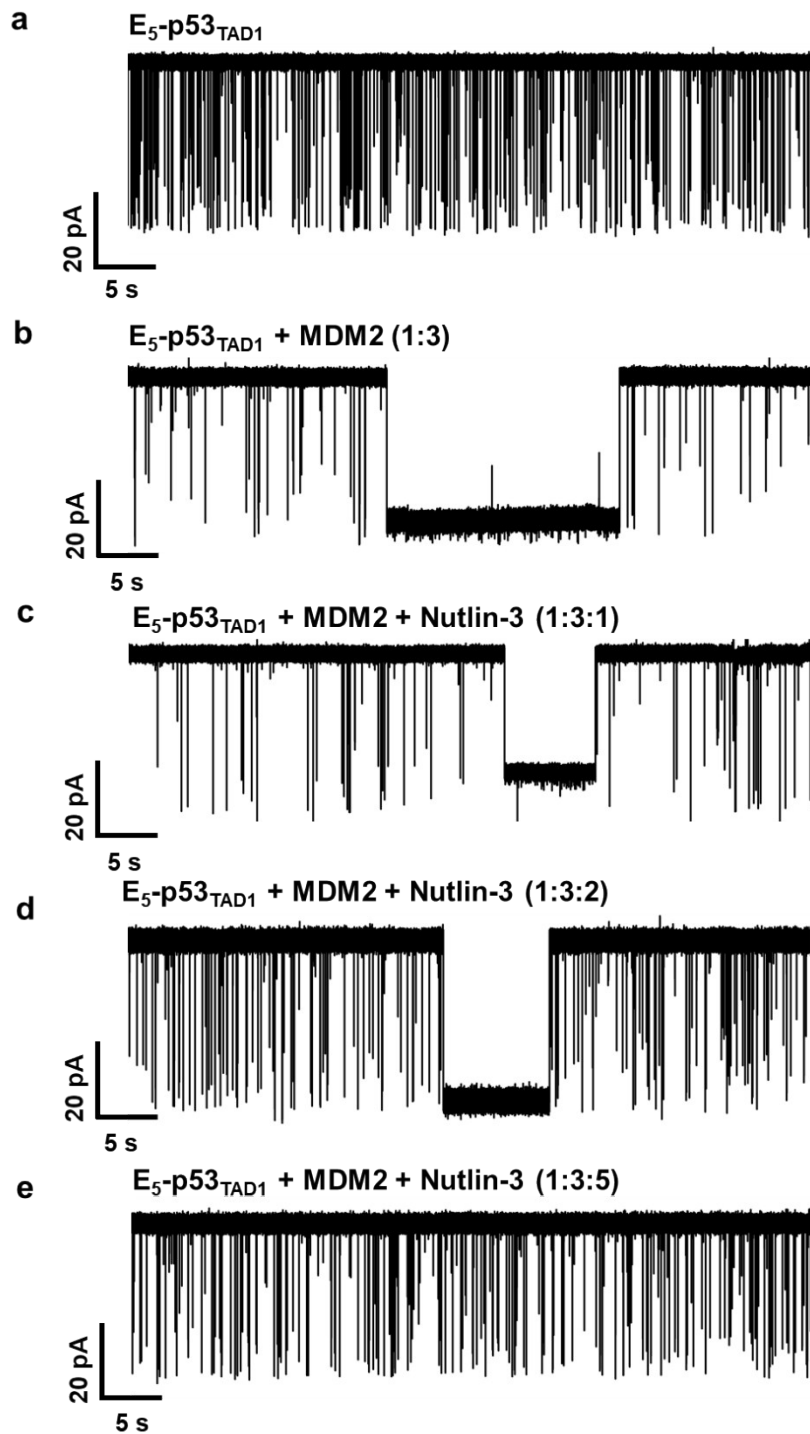


Fig. S8. Inhibitory effect of Nutlin-3 on the interaction between the E_5 -p53_{TAD1} and MDM2. Nanopore current traces of the E_5 -p53_{TAD1} (a), E_5 -p53_{TAD1}/MDM2 complex at the molar ratio of 1:3 (b), and E_5 -p53_{TAD1}/MDM2/Nutlin-3 complexes at the molar ratio of 1:3:1 (c), 1:3:2 (d) and 1:3:5 (e).

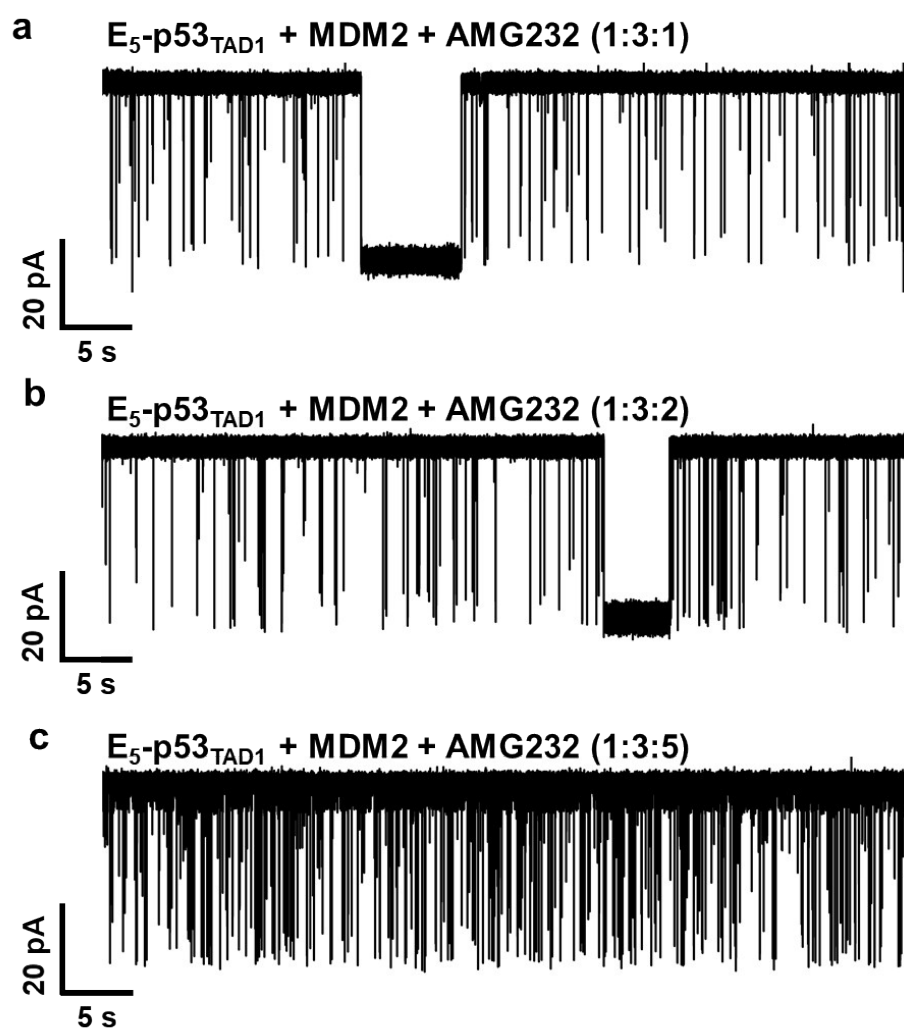


Fig. S9. Inhibitory effect of AMG232 on the interaction between the E₅-p53_{TAD1} and MDM2. Nanopore current traces of the E₅-p53_{TAD1}/MDM2/AMG232 complexes at the molar ratio of 1:3:1 (a), 1:3:2 (b), and 1:3:5 (c).

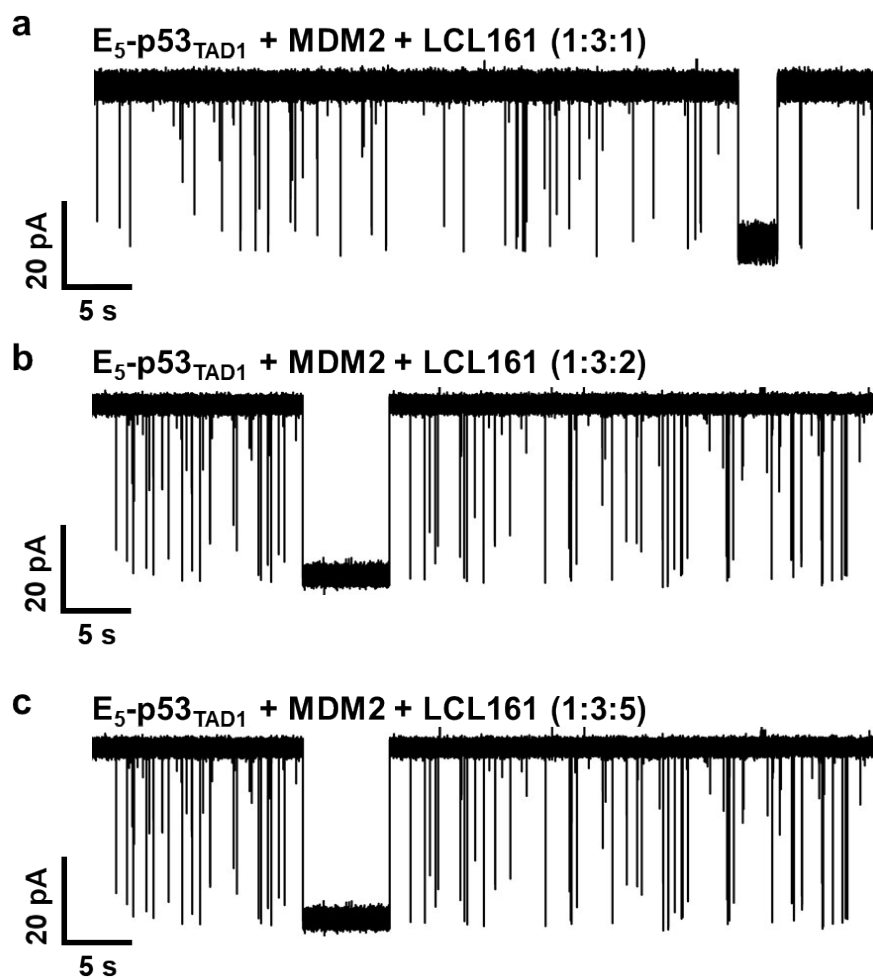


Fig. S10. Effect of the nonbinder control, LCL161 on the interaction between E_5 -p53_{TAD1} and MDM2. Nanopore current traces of the E_5 -p53_{TAD1}/MDM2 complexes with LCL161 at the molar ratio of 1:3:1 (a), 1:3:2 (b), and 1:3:5 (c).

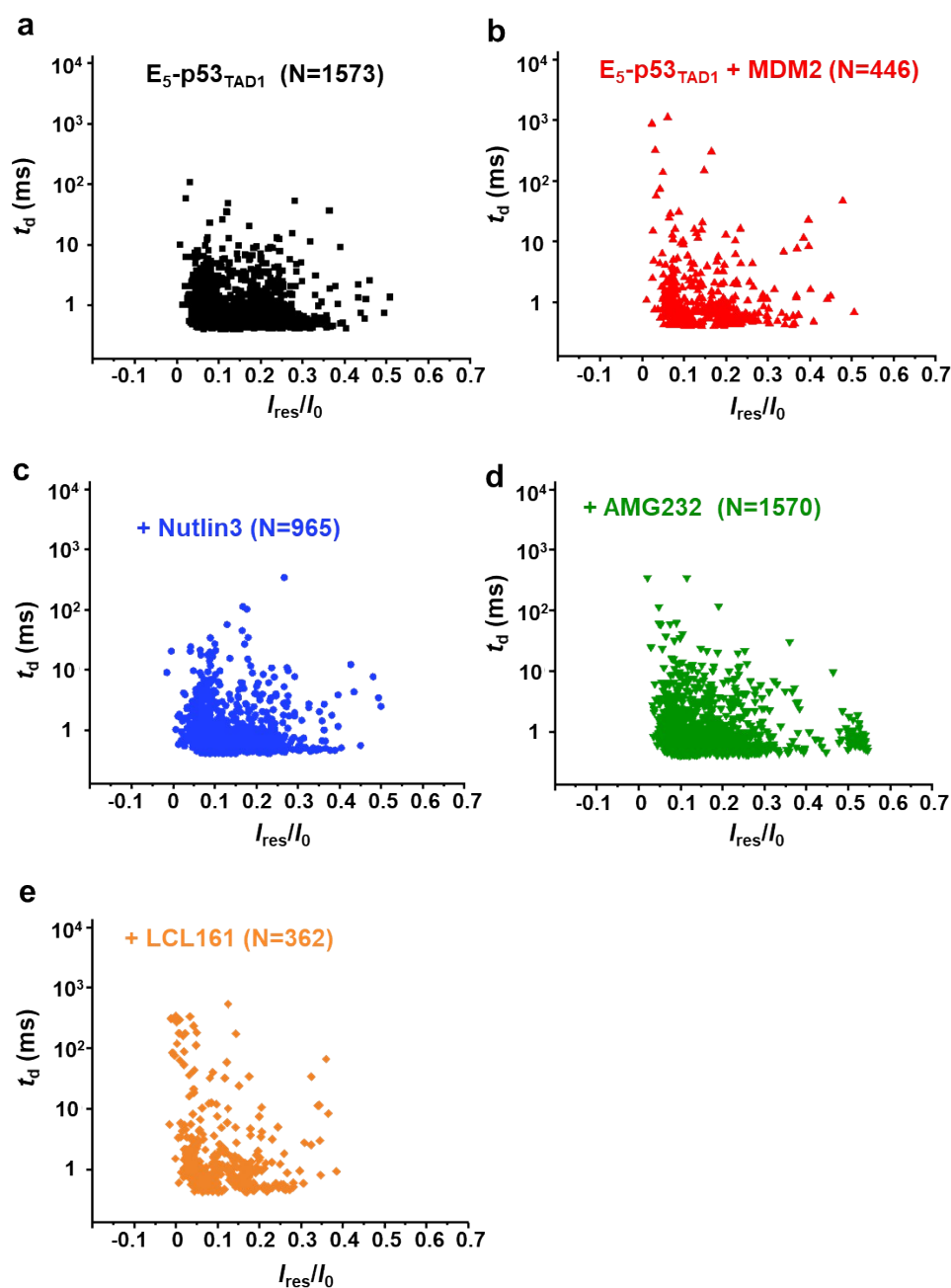


Fig. S11. Scatter plots of nanopore events of the E_5 -p53_{TAD1}/MDM2 complex in the absence and presence of small molecule inhibitors. Scatter plots of nanopore events obtained from free E_5 -p53_{TAD1} (a), the 1:3 E_5 -p53_{TAD1}/MDM2 complex (b), E_5 -p53_{TAD1}/MDM2 complexes in the presence of nutlin-3 (c), AMG232 (d), nonbinder LCL161 (e). Small molecule inhibitors were added to the complex at a molar ratio of 1:3:5. The represented scatter plots were analyzed for 10 min-nanopore current trace data. Nanopore measurements were performed at an applied voltage of 140 mV.

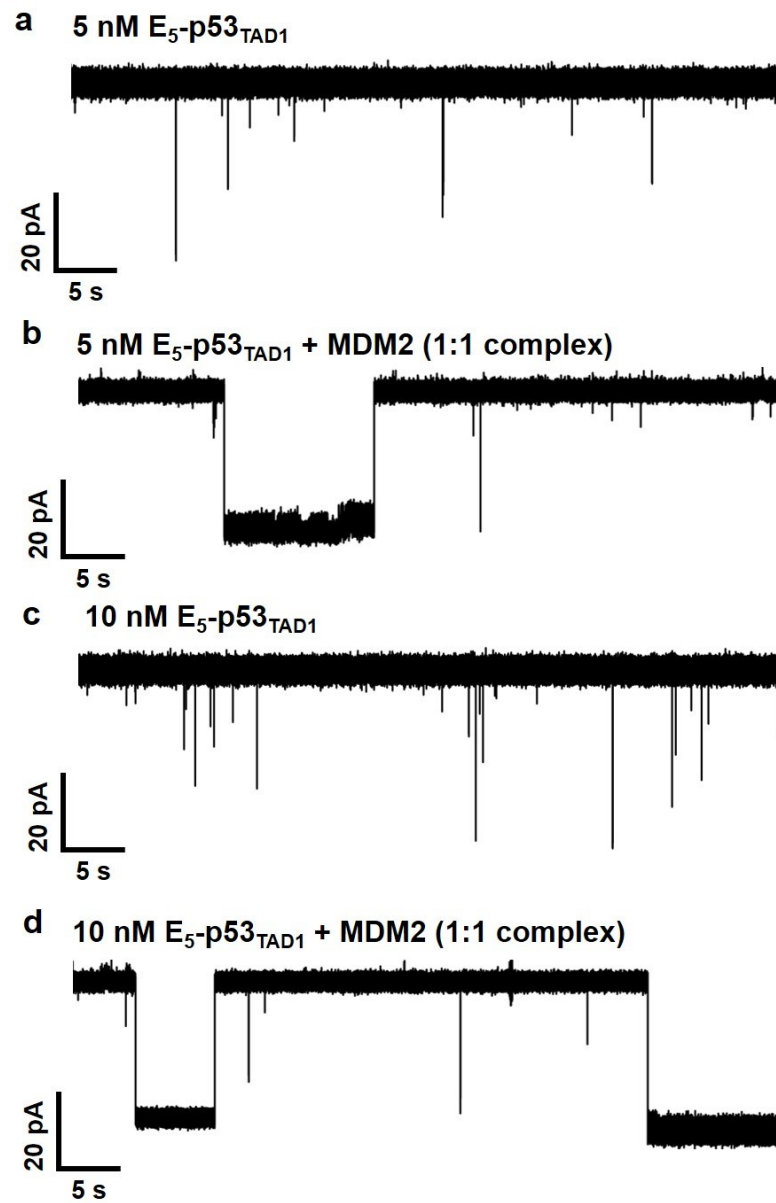


Fig. S12. Nanopore current traces of E_5 -p53_{TAD1} and 1:1 E_5 -p53_{TAD1}/MDM2 complexes at concentrations of 5nM (a–b) and 10nM (c–d). The minimum concentration of protein sample for aerolysin nanopore-based detection was 5nM.